Acoustics 2008
Geelong, Victoria, Australia 24 to 26 November 2008

Acoustics and Sustainability:

How should acoustics adapt to meet future demands?

Bearing calibration of the Cape Leeuwin hydroacoustic station

Binghui Li (1), Alexander Gavrilov (1) and Alec Duncan (1)

(1) Centre for Marine Science & Technology, Curtin University of Technology, Perth WA 6845, Australia

ABSTRACT

Calibration of bearing accuracy was conducted for the hydroacoustic station (HA01) deployed in the Indian Ocean off Cape Leeuwin, Western Australia, as part of the International Monitoring System of the Comprehensive Nuclear-Test-Ban Treaty. Both the random and systematic components of the bearing error were investigated using the azimuth measurement of various underwater events detected at the Cape Leeuwin station. The RMS value of the random component of azimuth estimation was examined using long-lasting low-frequency underwater events, such as harmonic tremor signals from drifting iceberg and seismic events including Sumatra earthquakes (main shock and aftershock). The random bearing errors were associated with horizontal deviation of hydrophones' moorings from the position based on a model of mooring motion. The systematic component was estimated through inversion of the signal travel time difference to the HA01 hydrophones from a number of underwater explosions made in the Indian Ocean at known locations. It is shown that the standard deviation of bearing estimates due to the random component is around 0.5 degree. The systematic error, which is about 0.8 degree clockwise, can be compensated by small correction of moorings' coordinates. Potential effects on azimuth estimation of horizontal refraction along cross-ocean acoustic propagation paths are also considered through numerical modelling.

INTRODUCTION

As part of International Monitoring System (IMS) of Comprehensive Nuclear-Test-Ban Treaty (CTBT), the Cape Leeuwin hydroacoustic station (HA01) was deployed about 150 km north-west of Cape Leeuwin, Western Australia. The station consists of three hydrophones (triplet) with horizontal spacing of around 2 km from one another. The hydrophones are submerged near the SOFAR acoustic channel axis at a depth of about 1100m. Because of its location and design, the station has the capability of long-range acoustic reception and bearing estimation. Since its deployment in 2001, the HA01 station has played an important role in monitoring various hydroacoustic events in the Indian and Southern Oceans, which include earthquakes and other tectonic activity, for example Indian Ocean ridge seismicity (Jeffrey and Roger, 2005&2006) and the Great Sumatra-Andaman Earthquake (Jeffrey and Roger, 2005; Tolstoy and DelWayne, 2006), as well as ice-related noise, such as noise produced by drifting icebergs (Emily et al, 2005; Jacques et al, 2006) and transient signals from ice breaking or rifting activities (Li and Gavrilov, 2006&2008; Gavrilov and Li, 2007&2008). In order to enhance the bearing accuracy of hydroacoustic monitoring, especially for the analysis of the localization and analysis of the spatial distribution of distant hydroacoustic events, it is essential to carry out the bearing calibration of the HA01 station.

Assuming both variable and permanent horizontal deviations of hydrophones' position from their nominal locations, the bearing error of Cape Leeuwin station was considered to consist of random and systematic components. Based on this assumption and using various underwater events detected at Cape Leeuwin station, both components of the bearing error were investigated. Potential effects of horizontal refraction along the acoustic propagation paths on the bearing accuracy were also examined through numerical modelling.

BEARING ERROR ANALYSIS

For the long-range hydroacoustic monitoring, the back-azimuths of observed hydroacoustic events at HA01 station can be estimated by the application of Plane Wave Fitting (PWF) method (Del Pezzo and Giudicepietro, 2002). The covariance matrix of the slowness vector $\mathbf{p}$ with two components (p_x, p_y) can also be derived as follows [Menke, 1984]:

$$\mathrm{cov}(\mathbf{p}) = [(\Delta\mathbf{x}^{\mathrm{T}}\Delta\mathbf{x})^{-1}\Delta\mathbf{x}]\mathrm{cov}(\mathbf{t})[(\Delta\mathbf{x}^{\mathrm{T}}\Delta\mathbf{x})^{-1}\Delta\mathbf{x}]^{\mathrm{T}}. \quad (1)$$

Where $\mathbf{t}$ is the vector of travel time differences between each pair of hydrophones $t_{i,j}$, and $\Delta\mathbf{x}$ is the vector of relative geometric positions of the hydrophones. Based on this equation, the standard deviation of the back-azimuth estimation can be obtained (Li and Gavrilov, 2006). From Eq. (1) we can see that the back-azimuth estimate via PWF is constrained by the errors of both the different travel time estimates $\mathbf{t}$ and relative position of hydrophones $\Delta\mathbf{x}$. The differential travel time estimates $t_{i,j}$ measured through cross-correlation of the signals at two receivers i and j depends on the quantization, the Signal-to-Noise Ratio (SNR), the signal bandwidth and its dura-

tion. In the case of remote hydroacoustic observation, the received signals for analysis are low-frequency intense broadband signals. Therefore, based on our previous study (Li and Gavrilov, 2006), the contributions of cross-correlation uncertainties to the travel time difference estimate, and consequently to the back-azimuth estimate, are negligible.

Apart from the contribution from the travel time difference estimates, the bearing errors are also caused by the deviation of the relative geometric positions of the hydrophones from the relative touchdown mooring position $\Delta\mathbf{x}$. The deviation may be due to the temporal horizontal motion of the hydrophones mounted on long vertical moorings, which has been thoroughly investigated in our previous study (Li and Gavrilov, 2006). We refer to the bearing error caused by this deviation component as random bearing error. Possible permanent deviation of the receivers' positions relative to their nominal locations may induce a time-independent or systematic bearing error. Although the systematic bearing error is superimposed on the random bearing errors, it can be estimated statistically given the exact bearings of enough known sample events. Based on the observation of a number of underwater explosions with know positions, the systematic bearing error of HA01 will be explored by the inversion of relative deviations of receivers using modelled and measured travel time differences between pairs of receivers.

RANDOM BEARING ERROR ESTIMATION

Hydroacoustic recordings over six years, from December 2001 to January 2008 have so far been collected from the HA01 station. These continuous sea noise recordings were divided into 20-second fragments and only the fragments with high coherence at three receivers were selected for further analysis. The cross-correlation between noise signals on any pair of hydrophones must exceed a threshold of 0.5 in at least one of four different frequency bands: 3-15 Hz, 15-30 Hz, 30-60 Hz, and 60-100 Hz. Based on characteristics of the waveform and spectrogram of these selected signals, the coherent events were divided into different classes. Among them is the group of harmonic tremor signals which is characterized by a fundamental frequency below 10 Hz with several harmonics at higher frequencies. Tremor events have various durations from tens of minutes to several hours or even longer. These events are believed to be related to drifting icebergs. Signals from seismic events, such as earthquakes, display extremely high energy concentration at very low frequencies below 5 Hz, and the duration of the signals can be from days up to months. Based on the duration and the high SNR in the low frequency band, a number of tremor and seismic events were selected for the estimation of HA01 random bearing error, as shown in Table 1. In the selection process, only stationary sections of those events, when the mean value of measured back-azimuth did not change, were considered.

Table 1. The azimuthal mean values and the standard deviations (SD) of six long-lasting Antarctic tremor events and four seismic events. TR: tremor event; SE: seismic event; MS and AS: the main shock and the aftershock of the Great Sumatra-Andaman Earthquake; Mean and SD represent the mean value and standard deviation of azimuth respectively.

Events	Lasting time [year/day]	Mean [^{0}]	SD [^{0}]
TR 1	02/151.54 ~ 02/152.36	163.927	0.09
TR 2	03/217.38 ~ 03/217.46	162.740	0.16
TR 3	04/170.14 ~ 04/170.88	195.571	0.18
TR 4	05/061.83 ~ 05/075.11	180.242	0.19
TR 5	06/003.87 ~ 06/004.65	181.952	0.09
TR 6	07/214.75 ~ 07/224.07	191.770	0.11
SE 1	03/233.54 ~ 03/367.50	121.254	0.40
SE 2	07/273.25~ 08/009.30	128.086	0.31
SE 3 (MS)	04/361 ~ 05/010	331.560	0.65
SE 4 (AS)	05/087 ~ 05/101	333.274	0.24

For the six selected tremor signals with azimuths ranging from ~160 to ~200 degrees, the standard deviation of azimuth estimates is mostly below 0.2 degrees. If compared with the modelled result shown in Fig. 3 in the reference [Li and Gavrilov, 2006], such small values of the standard deviation correspond to only a few metres deviation of the HA01 hydrophones from their nominal position. The standard deviation values of azimuth estimates of the four earthquake events, including two events from the Southern Ocean and another two from the main shock and aftershock of the Great Sumatra-Andaman Earthquake, are larger than those values from the tremor events. This is expected considering that the dimension of the region of those seismic events is larger than that of ice-related events. If we attribute the azimuth variation due to the dimension of seismic events to that from the hydrophones' deviation, even in the extreme scenario as in the mainshock of great Sumatra-Andaman Earthquake, the SD of azimuth measurement is only as much as 0.65 degree, which correlates with slightly over 10 m SD of horizontal motion for each HA01 hydrophone. Therefore based on the analysis of SD value of measured azimuth from both tremor and earthquake events shown in Table 1, it can be concluded that the random bearing error of HA01 is less than half a degree, which is consistent with our previous preliminary result [Gavrilov and Li, 2007].

SYSTEMATIC BEARING ERROR ESTIMATION

Based on a simple geometric model described in Appendix 1, the horizontal deviation of the hydrophones relative to their nominal position in Cartesian coordinate system can be expressed by Eq. (A8), providing a number of calibration events with their exact coordinate.

Blackman proposed some experiments aimed at calibrating

Table 2. The sources of underwater acoustic explosions and their shot times, coordinates, shot depths, original and measured azimuths from HA01, inverted group velocities and the azimuth residual values. The azimuth residual is the value of measured azimuth minus predicted azimuth using HA01 receivers' mooring coordinates.

Sources of Explosion	Shot time [year/day/hour]	Coordinates [latitude longitude]	Shot Depth (m)	Original Azimuth [^{o}]	Group Velocity (km/s)	Measured Azimuth [^{o}]	Azimuth Residual [^{o}]
A6 SUS3	03/149/04.3394	[-22.0848 72.7422]	915	278.18	1.472	278.62	0.44
A7 SUS3	03/151/11.8699	[-18.4374 80.9182]	915	290.38	1.466	291.69	1.31
A8 SUS2A	03/152/09.2333	[-17.1759 83.6751]	610	295.13	1.467	296.11	0.98
A10 SUS3	03/158/03.9227	[-12.2133 96.7966]	915	320.85	1.464	321.69	0.84
A11 SUS	03/160/00.6261	[-13.1980 104.6944]	915	336.05	1.466	337.52	1.47
Bengal Bay 1	04/126/15.4678	[10.14 89.07]	-	327.33	1.466	327.94	0.61
Bengal Bay 2	04/126/16.2794	[10.01 89.50]	-	327.75	1.467	328.41	0.67

the CTBT hydroacoustic stations in the Indian Ocean and some of them have been implemented in the past few years [Blackman et al, 2003, 2004, 2005 and 2007]. Due to high transmission loss and some data missing in the HA01 recordings, only signals from 5 SUS explosions, made in 2003 during the cruise of R/V Melville across the Indian Ocean from Cape Town, South Africa to the Cocos Islands [Blackman et al, 2003], were detected at HA01 with sufficient SNR to be used for bearing calibration. The recordings of two strong explosions made in the Bay of Bengal on May 5, 2004 at known coordinates [Roger et al, 2005] were also used for calibration. The sources of the seven calibration events, and their shot times, coordinates, shot depths and azimuths from HA01 are shown in the first five columns of Table 2. All of these explosions were made in deep water regions and the signals from these explosions underwent multi-path propagation in the SOFAR acoustic channel. To account for multi-path propagation effects, a Progressive Multi-Channel Correlation (PMCC) method [Cansi, 1995] was used for measuring the signal travel time difference to the HA01 hydrophones needed for slowness and back-azimuth estimates by the plane wave fitting algorithm. In the PMCC method, the correlation of signals at three receivers *i*, *j*, *k*, is calculated within sliding windows and in a series of frequency bands to obtain the consistency of the following criterion:

$$r_{ijk} \equiv \Delta t_{ij} + \Delta t_{jk} + \Delta t_{ki} = 0 \qquad (3)$$

Where Δt_{ij} is the time delay between the arrivals of a signal at receivers *i* and *j*. Due to the background noise and the finite sampling rate, the consistency condition in Eq. (3) might have slight deviation from zero for fully coherent signals. Therefore we set a threshold of the consistency of 0.02 s. Signals filtered in different frequency bands were considered to be suitable for azimuth estimation, if the consistency criterion did not exceed this threshold. The waveform of the calibration event arrivals has a relatively short and sharp peak and, therefore, a single time window of about one second long was selected for the correlation analysis, rather than a series of sliding windows. The passband of 20 Hz was selected for the sliding frequency window, and was applied in the frequency range from 10 Hz to 70 Hz, thus excluding the frequency bands where the coherence of background noise was high. As additional criteria for signal acceptance, the cross correlation coefficient was tested to be at least 0.5 and the group velocity estimates to be within 1.40 - 1.50 km/s. The inverted group velocities, azimuths and the difference of the measured and actual azimuths are shown in the last three columns of Table 2. Note that the measured back-azimuths to all seven calibration events have a small clock-wise deviation from their actual values.

Fig. 1 shows the HA01 triplet patterns before and after the relative coordinate calibration in the Cartesian coordinate system. The size of the calibrated triplet pattern is inversely proportional to the sound speed in the geometric model as demonstrated in Appendix 1. To draw the corrected triplet pattern shown in Fig. 1, the sound speed was set to be the mean value of the inverted group velocities given in the 6th column of Table 2. After calibration, the shape of the HA01 triplet appeared to be anti-clockwise rotated relative to the original pattern. Using the original and calibrated HA01 triplet coordinates, the systematic bearing error was calculated as a function of azimuth, which is shown in Fig. 2. The systematic error is slightly azimuth dependent and the average clockwise deviation is around 0.8 degree.

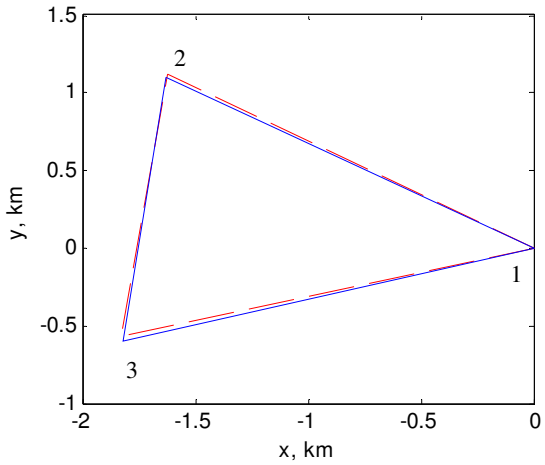

Figure 1. The patterns of the HA01 triplet in the Cartesian coordinate system before and after correction. The blue line represents the pattern based on the relative positions of the moorings determined during deployment; the red line is the result obtained after the relative coordinate calibration. The coordinates of hydrophone one were set as the reference position.

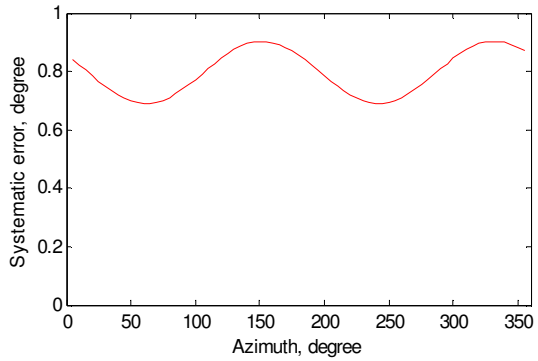

Figure 2. Systematic bearing error as the function of azimuth calculated based on the original and calibrated relative coordinates of HA01 triplet.

AN ANTARCTIC ICEBERG COLLISION OBSERVATION

A series of harmonic tremor signals from late Julian day 260 till middle of Julian day 262 in 2003 was observed at HA01. The back-azimuth to these events was calculated before and after correction of the HA01 relative triplet coordinates, which is shown in Fig. 3. One can see the calibration offset of around 1.2^0 from the original bearing estimates. Over the 1.5-day observation period the mean value of calibrated azimuths to the observed tremor events varied gradually from 163^0 to 163.7^0 with the standard deviation of 0.2^0.

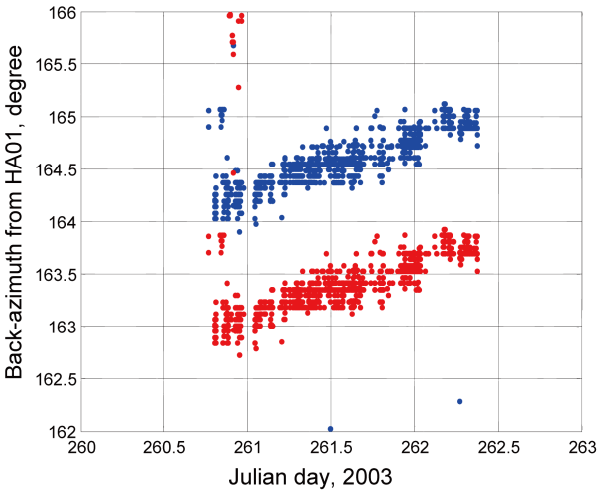

Figure 3. The back-azimuth to a series of harmonic tremor signals received at HA01 as the function of signal arrival times. Blue and red dots represent the azimuth measured using original and corrected relative coordinates of the HA01 triplet respectively.

An investigation of Antarctic iceberg activity for this time period and the area on the Antarctic continental shelf that corresponded to the measured azimuth was conducted using the Antarctic Iceberg Tracking Database (http://www.scp.byu.edu/data/iceberg/database1.html). The observed tremor signals are believed to be generated by collisions of iceberg C008 with the ice shelf off Victor Bay. This iceberg has been tracked from the middle of 1999 to early 2008 using satellite images, during which time it has drifted along almost half of the Antarctic coastline from the Commonwealth Bay to the Weddell Sea. Fig. 4 shows the locations of iceberg C008 at different times and the bearing lines (bars) from HA01 drawn for the original and corrected azimuth estimates as shown in Fig. 3. Remarkably, the back-azimuth to these events estimated after correction of the HA01 triplet position, indicates exactly the part of the ice shelf edge that the iceberg C008 drifted by and most likely collided with on Julian day 261, whereas the back-azimuth derived from the original position of HA01 indicates at the region where C008 was observed on Julian day 268. According to the overall variation of the azimuth and the duration of this series of tremor signals, the total range that iceberg C008 had drifted, scraping the ice shelf, was about 35.6 km with an average drifting speed of 0.93 km per hour.

This observation is further evidence for the systematic bearing error.

EFFECT OF HORIZONTAL REFRACTION ON BEARING ESTIMATION

To examine all possible errors in locating remote underwater acoustic events by the CTBT stations, it is necessary to investigate the effect on the bearing estimation of horizontal refraction of sound propagation in the ocean. Both large-scale spatial variations of oceanographic characteristics and changes in the bottom topography can induce horizontal refraction [Jensen et al, 2000; Doolittle et al, 1988]. In this study, we followed the computational procedure proposed for the analysis of the Perth-Bermuda propagation experiment results [Heaney et al, 1991]. It involves the combination of an adiabatic mode theory in the vertical dimension and a ray theory in the horizontal dimension and, therefore, takes into account horizontal refraction of individual modes due to both transverse sound speed gradients and bottom interaction over the continental slopes and sea mounts. The ray model was constructed on the surface of the Earth represented by an ellipsoid of rotation and expressed in terms of the parameters ϕ, λ, and α, where ϕ and λ are the latitude and longitude respectively, and α the azimuth angle measured clockwise from the north. The ray equations on an ellipsoid are:

$$\dot{\phi} = \cos\alpha / \mu(\phi) \tag{4a}$$

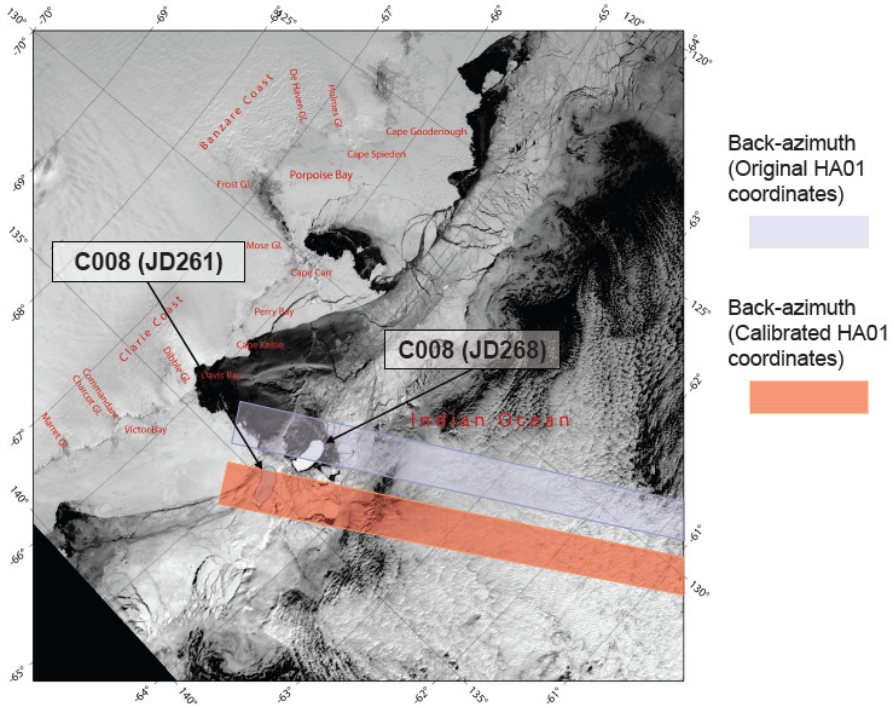

Figure 4. A satellite image showing the location iceberg C008 drifted along the ice shelf off Victor Bay on Julian days 261 and 268 in 2003. The blue and red bars are the regions seen along the back-azimuths to the tremor signals measured before and after correction of the HA01 triplet position respectively.

$$\dot{\lambda} = \sin\alpha / v(\phi)\cos\phi \tag{4b}$$

$$\dot{\alpha} = \frac{\sin\alpha}{v(\phi)}\tan\phi - (\frac{\sin\alpha}{\mu(\phi)}\frac{\partial}{\partial\phi} - \frac{\cos\alpha}{v(\phi)\cos\phi}\frac{\partial}{\partial\lambda})\log\kappa_n \tag{4c}$$

where κ_n are the horizontal wavenumbers of modes and the variables μ and v are:

$$\mu(\phi) = r_{eq}(1-\varepsilon^2)/(1-\varepsilon^2\sin^2\phi)^{3/2}$$

$$v(\phi) = r_{eq}(1-\varepsilon^2\sin^2\phi)^{1/2} \tag{5}$$

and r_{eq} and ε are the equatorial radius and eccentricity of the Earth respectively. The last term in Eq. (4c) accounts for distortion of the ray paths due to gradients of the horizontal wavenumber κ_n based on the Snell's law. If this term is neglected, the solutions of Eq. (4) are geodesics on the ellipsoid [Bomford, 1980, P649].

The modal horizontal wavenumbers were calculated using the KRAKEN program [Porter and Reiss, 1984] on a horizontal grid with the grid size of half degree. The sound speed profiles were derived from climatology salinity and temperature data gridded to 1-degree resolution in the World Ocean Atlas 2005 [Locarnini et al and Antonov et al, 2006] and then interpolated into a half-degree grid. The bathymetry data were taken from the ETOPO2 Global 2-Minute Gridded Elevation Data (http://www.ngdc.noaa.gov/mgg/fliers/01mgg04.html). The system of ordinary differential equations Eq. (4) can be solved using a 4-th or 5-th order Runge-Kutta method [Williams et al, 2007]. During the integration process, the grid size of the modal wavenumbers was set to be equal to the maximum integration step to reduce numerical integration errors.

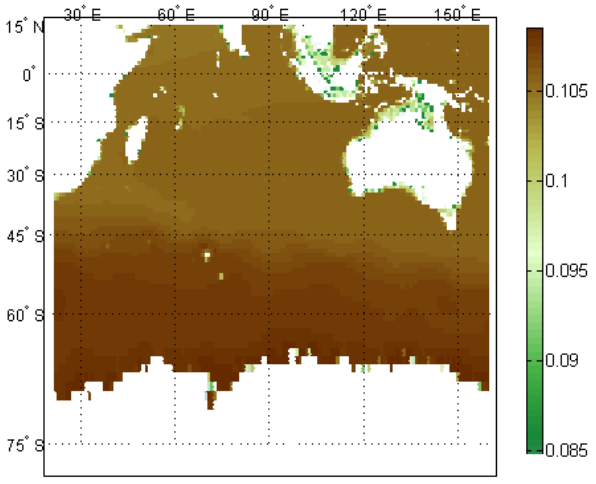

Figure 5. The map projection of the mode 1 horizontal wavenumber matrix in the region of Indian and Southern Oceans. The frequency is at 20 Hz and climatological data are taken for the winter season.

Fig. 5 shows the map projection of the matrix of mode 1 wavenumbers at 20 Hz in the winter season. As can be seen, in deep water regions, the wavenumber has strong dependence on the sound speed profile rather than bathymetry. In the Indian Ocean north of the Antarctic Convergence Zone (ACZ), the wavenumber is almost uniform except for the region around the equator. The strongest gradient of the wavenumber is in the ACZ, across which the sound speed profile evolves from the polar upward-refracting shape in Southern Ocean to the temperate ocean shape with a deep SOFAR channel in the temperate ocean. The water depth is much shallower over the Antarctic continental shelf, and hence the modal wavenumber undergoes noticeable dependence on depth.

Fig. 6 gives the one-degree resolution map of bearing deviation at HA01 due to horizontal refraction in the Indian Ocean, across the ACZ and in the Southern Ocean region over the Antarctic continental shelf, numerically modelled using the horizontal wavenumber matrix shown in Fig. 5. The bearing deviation from the geodetic azimuth at each grid point was calculated as the residual $\Delta\theta = \theta_1 - \theta_2$, where θ_1 is the true azimuth to the grid point as seen from HA01 and θ_2 is the back azimuth to the end point of the refracted ray derived from Eq.(4) for the same launch angle. The ray has the same length as the geodesic. The bearing deviation induced by horizontal refraction for the most part of Indian Ocean region north of ACZ does not exceed 0.2^0 because of small gradients of the wavenumber. Strong wavenumber gradients across the ACZ introduce considerable azimuth dependent deviation of the acoustic propagation path to the locations within the ACZ and south of it. The azimuth deviation in the Southern Ocean south of the ACZ has both negative values in the western region and positive values in the eastern region with a transition zone around the azimuth of about 203^0 from HA01, along which the propagation path is nearly perpendicular to the ACZ.

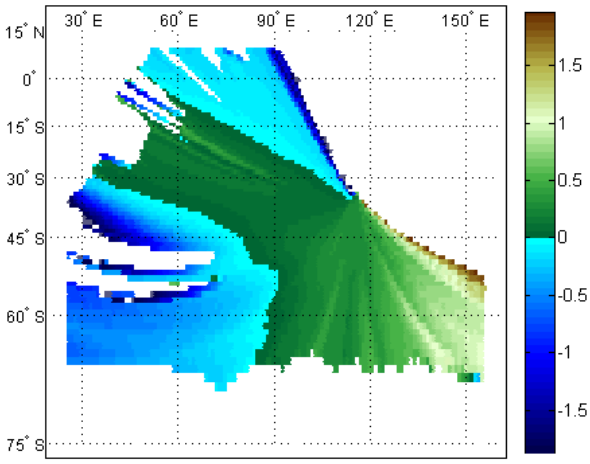

Figure 6. The map projection of bearing deviation at the HA01 receiving station for noise sources located in the Indian and Southern Oceans. Deviation is due to horizontal refraction calculated for the horizontal wavenumber matrix shown in Fig. 5.

The dependence of the wavenumber gradient on mode number and frequency was investigated for the Southern Ocean region. It is found that 1) for a certain mode, the gradient of the horizontal wavenumber κ_n across the ACZ increases with frequency and 2) for a fixed frequency, the gradient decreases with mode number. Such dependence takes place because higher order modes at lower frequencies penetrate deeper in the water column and hence they are less sensitive to rapid change in the sound speed in the upper water layer across the ACZ.

CONCLUSIONS

In this paper, bearing errors of the HA01 station for long-range low-frequency hydroacoustic monitoring are considered to contain a systematic component in addition to the

random one due to motion of the HA01 hydrophones. The systematic component results from the limited accuracy of positioning of the HA01 moorings that was performed after deployment. An analysis of a number of long-lasting, low-frequency underwater harmonic tremor signals and seismic events, as well as some signals from explosions made in the Indian Ocean at known locations was conducted for bearing calibration of the HA01 station. It is demonstrated that the random component of HA01 bearing errors due to motions of the receivers is below half a degree, which is in agreement with the estimates made before, while the systematic component is around 0.8 degrees. The horizontal refraction effect also contributes considerably to HA01 bearing errors for the Ocean region within and beyond the ACZ. The effect is azimuth dependent. All these bearing errors must be taking into account when locating ice events using CTBT hydroacoustic stations.

APPENDIX A

A simple geometric model for HA01 bearing calibration

This analysis is made in the Cartesian coordinate system by projecting coordinates from the Geodetic Earth Model. Under the condition that the underwater explosions are far enough from the hydroacoustic station, the propagation paths can be represented in the horizontal coordinates *x* and *y* ignoring the depth difference. Let the coordinates of mooring 1 of the HA01 triplet, (x_1^0 , y_1^0), be a reference position for both original and corrected systems, and the relative coordinates of moorings two and three are (x_2^0 , y_2^0) and (x_3^0 , y_3^0) respectively. Let also the coordinates of the *n*-th underwater explosive event be (x_r^n , y_r^n). The corrected relative coordinates of moorings 2 and 3, (x_2 , y_2) and (x_3 , y_3) respectively, have deviations (δx_2 , δy_2) and (δx_3 , δy_3) from the original positions. The travel time differences T_{ij}^n from the *n*th explosion to a pair of hydrophones *i* and *j*, can be expressed as a function of the vector of deviations $\tilde{\delta} = (\delta x_2, \delta y_2, \delta x_3, \delta y_3)^{\mathrm{T}}$ as:

$$T_{ij}^n = f_{ij}^n(\tilde{\delta}) \quad i, j = 1,2,3 \;\&\; i \neq j \;, \tag{A1}$$

where the subscript T denotes the matrix transpose operation. If the deviations of hydrophones from the original positions are small compared with the dimension of the triplet, the travel time differences T_{ij}^n can be expanded in a power series of deviations from the original coordinates and only the first two low-order terms of the expansion can be kept:

$$T_{ij}^n = f_{ij}^n(\tilde{\delta}^0) + \left.\frac{\partial f_{ij}^n}{\partial(\delta x_2)}\right|_{\tilde{\delta}^0} \delta x_2 + \left.\frac{\partial f_{ij}^n}{\partial(\delta y_2)}\right|_{\tilde{\delta}^0} \delta y_2 + \left.\frac{\partial f_{ij}^n}{\partial(\delta x_3)}\right|_{\tilde{\delta}^0} \delta x_3 + \left.\frac{\partial f_{ij}^n}{\partial(\delta y_3)}\right|_{\tilde{\delta}^0} \delta y_3 \tag{A2}$$

where the original deviations $\tilde{\delta}^0 \equiv (\delta x_2^0, \delta y_2^0, \delta x_3^0, \delta y_3^0)$ are set to be a zero vector.

The formula for the residuals of the travel time difference can be obtained from (A2):

$$T_{ij}^n - f_{ij}^0(\tilde{\delta}^0) = \left.\frac{\partial f_{ij}^n}{\partial(\delta x_2)}\right|_{\tilde{\delta}^0} \delta x_2 + \left.\frac{\partial f_{ij}^n}{\partial(\delta y_2)}\right|_{\tilde{\delta}^0} \delta y_2 + \left.\frac{\partial f_{ij}^n}{\partial(\delta x_3)}\right|_{\tilde{\delta}^0} \delta x_3 + \left.\frac{\partial f_{ij}^n}{\partial(\delta y_3)}\right|_{\tilde{\delta}^0} \delta y_3 \tag{A3}$$

In the matrix notation, one can express (A3) as:

$$Y^n = A^n \cdot \tilde{\delta} \tag{A4}$$

where the vector of the residual of the travel time difference is

$$Y^n = [\, T_{21}^n - f_{21}^n\big|_{\tilde{\delta}^0} \;\; T_{31}^n - f_{31}^n\big|_{\tilde{\delta}^0} \;\; T_{23}^n - f_{23}^n\big|_{\tilde{\delta}^0} \,]^{\mathrm{T}} \tag{A5}$$

and A^n is a 3×4 matrix of derivatives of the travel time difference. Therefore, for total *N* explosive events, the following equation can be obtained:

$$Y = A \cdot \tilde{\delta} \tag{A6}$$

where *Y* is a one-column vector with 3*N* elements, and A is a 3*N*×4 matrix:

$$Y = [Y^1\; Y^2 \ldots Y^n]^{\mathrm{T}}; \quad A = [A^1\; A^2 \ldots A^n]^{\mathrm{T}} \tag{A7}$$

Then the least square solution of $\tilde{\delta}$ can be obtained:

$$\tilde{\delta} = [A^T A]^{-1} A^T Y \tag{A8}$$

Assuming the sound speed along the propagation path to be constant *v* km/s, the travel time differences between the HA01 hydrophones from *n*th explosive events can be calculated as:

$$T_{21}^n = f_{21}^n(\tilde{\delta}) = \frac{1}{v}\left(\sqrt{x_r^{n\,2} + y_r^{n\,2}} - \sqrt{(x_r^n - x_2 - \delta x_2)^2 + (y_r^n - y_2 - \delta y_2)^2}\right) \tag{A9}$$

$$T_{31}^n = f_{31}^n(\tilde{\delta}) = \frac{1}{v}\left(\sqrt{x_r^{n\,2} + y_r^{n\,2}} - \sqrt{(x_r^n - x_3 - \delta x_3)^2 + (y_r^n - y_3 - \delta y_3)^2}\right) \tag{A10}$$

$$T_{23}^n = f_{23}^n(\tilde{\delta}) = \frac{1}{v}\left(\sqrt{(x_r^n - x_2 - \delta x_2)^2 + (y_r^n - y_2 - \delta y_2)} - \sqrt{(x_r^n - x_3 - \delta x_3)^2 + (y_r^n - y_3 - \delta y_3)^2}\right) \tag{A11}$$

ACKNOWLEDGEMENTS

The authors thank Dr. David Jepsen of Geoscience Australia for providing us with the HA01 acoustic data and Dr. Donna K. Blackman of IGPP, Scripps Institution of Oceanography for providing NBP0701 Hydroacoustics Project Cruise Report.

REFERENCES

Antonov J.I., R.A. Locarnini, T.P.Boyer, A.V.Mishonov, H.E.Garcia, 2006, *World Ocean Atlas 2005, Volume 2: Salinity.* S. Levitu, Ed. NOAA Atlas NESDIS 62, U.S. Government Printing Office, Washington D.C., 182 pp.

Bomford G., 1980, *Geodesy*, Oxford University Press, 885pp.

Brian P.Flannery, 2007, *Numerical Recipes - The art of scientific computing*, Third Edition, Cambridge University Press, 1262pp.

Cansi, Y., 1995, *An automatic seismic event processing for detection and location: the P.M.C.C. method*, Geophysical Resesarch Letters 22(9): 1021-1024.

Del Pezzo Edoardo and F. Giudicepietro, 2002, *Plane wave fitting method for a plane, small aperture, short period seismic array: a MATHCAD program*, Computers&Geosciences 28: 59-64.

Donna K. Blackman and C. D. d. Groot-Hedlin, 2005, *Acoustic propagation through the antarctic convergence zone-calibration tests for the nuclear test monitoring system*, 27th Seismic Research Review: Ground-Based Nuclear Explosion Monitoring Technologies, Rancho Mirage, California.

Donna K. Blackman and C. Scott Jenkins, 2007, *NBP0701 Hydroacoustics Project Cruise Report*.

Donna K. Blackman, Catherine D. de Groot-Hedlin, Phil Harben, Allan Sauter and John A. Orcutt, 2004, *Testing low/very low freqeuncy acoustic sources for basin-wide propagation in the Indian Ocean*, J.Acoust.Soc.Am 116(4): 2057-2066.

Donna K. Blackman, James A. Mercer, Rex Andrew, Catherine D. de Groot-Hedlin, and Philip E. Harben, 2003, *Indian Ocean calibration tests: Cape Town-Cocos Keeling 2003*, 25th Seismic Research Review - Nuclear Explosion Monitoring: Building the Knowledge Base, Tucson, Arizona.

Emily Chapp, DelWayne. R. Bohnenstiehl and Tolstoy M, 2005, *Sound-channel Observations of Ice-generated Tremor in the Indian Ocean*, Geochemistry, Geophysics and Geosystems 6(Q06003, doi: 10.1029/2004GC000889).

Finn B. Jensen, William A. Kuperman, Michael B. Porter and Henrik Schmidt, 2000, *Computational Ocean Acoustics*, New York, Springer.

Gavrilov, A., Li, B. ,2008**,** *Long-term variations of ice breaking noise in Antarctica***,** Proceedings of Acoustics '08, Paris, 29 June - 4 July 2008. ISBN 978-2-9521105-4-9.

Gavrilov, A., Li, B., 2007, *Antarctica as one of the major sources of noise in the ocean*, Underwater Acoustic Measurements: Technologies & Results, 2nd International Conference and Exhibition, Heraklion, Crete, 25-29 June 2007. Abstract. ISBN 978 960 88702-5-3.

J. Roger Bowman, Jeffrey A. Hanson and David Jepsen, 2005, *An Active-source Hydroacoustic Experiment in the Indian Ocean*, 27th Seismic Research Review: Ground-Based Nuclear Explosion Monitoring Technologies, Rancho Mirage, California.

Jacques Talandier, Olivier Hyvernaud, Dominique Reymond and Emile A. Okal, 2006, *hydroacoustic signals generated by parked and drifting icebergs in the Southern Indian and Pacific Oceans*, Geophys. J. Int, 165: 817-834.

Jeffrey A. Hanson and J. Roger Bowman, 2005, *Dispersive and reflected tsunami signals from the 2004 Indian Ocean tsunami observed on hydrophones and seismic stations*, Geophysical Resesarch Letters 32 (L17606, doi:10.1029/2005GL023783).

Jeffrey A. Hanson and J. Roger Bowman, 2005, *Indian Ocean ridge seismicity observed with a permanent hydroacoustic network*, Geophysical Resesarch Letters 32 (L06301, doi:10.1029/2004GL021931).

Jeffrey A. Hanson and J. Roger Bowman, 2006, *Methods for monitoring hydroacoustic events using direct and reflected T waves in the Indian Ocean*, Journal of Geophysical Research 111(B02305, doi:10.1029/2004JB003609).

K. D. Heaney, W.A.Kuperman and B.E. McDonald, 1991, *Perth-Bermuda sound propagation (1960): Adiabatic mode interpretation*, J.Acoust.Soc.Am 90(5): 2586-2594.

Li, B., Gavrilov, A., 2006, *Hydroacoustic Observation of Antarctic Ice Disintegration Events in the Indian Ocean*, First Australasian Acoustical Societies' Conference, Acoustics 2006: Noise of Progress, pp 479-484, Christchurch New Zealsnd, 20-22 November 2006. ISBN 978-0-909885-25-9. ISSN 1446-0998.

Li, B., Gavrilov, A., 2008, *Localization of Antarctic ice breaking events by frequency dispersion of the signals received at a single hydroacoustic station in the Indian Ocean*, Proceedings of Acoustics '08, Paris, 29 June - 4 July 2008. ISBN 978-2-9521105-4-9.

Menke W., 1984, *Geophysical Data Analysis: Discrete Inverse Theory*, New York, Academic Press.

Michael B. Porter and E. L. Reiss, 1984, *A Numerical Method for Ocean-Acoustic Normal Modes*, J.Acoust.Soc.Am 76: 244-252.

R. Doolittle, A.Tolstoy and M.Buckingham, 1988, *Experimental confirmation of horizontal refraction of CW acoustic radiation from a point source in a wedge-shaped ocean environment*, J.Acoust.Soc.Am 83: 2117-2125.

Tolstoy Maya and DelWayne R. Bohnenstiehl, 2006, *Hydroacoustic contributions to understanding the December 26th 2004 great Sumatra-Andaman Earthquake*, Surv Geophys 27: 633-646.

William H.Press, Saul A.Teukolsky, William T.Vetterling,